

Synthesis, Nicotinic Acetylcholine Receptor Binding Affinities, and Molecular Modeling of Constrained Epibatidine Analogues

Zhi-Liang Wei,[†] Pavel A. Petukhov,[†] Yingxian Xiao,[‡] Werner Tückmantel,[†] Clifford George,[§] Kenneth J. Kellar,[‡] and Alan P. Kozikowski^{*,†}

Drug Discovery Program, Department of Neurology, Department of Pharmacology, Georgetown University Medical Center, 3900 Reservoir Road, NW, Washington, D.C. 20057, and Naval Research Laboratory, 4555 Overlook Avenue, SW, Washington, D.C. 20375

Received November 18, 2002

Abstract: Conformationally constrained epibatidine analogues **20a,b** and **23a,b** were synthesized using a radical cyclization as the key step. Radioligand displacement assays to six defined rat nicotinic acetylcholine receptor (nAChR) subtypes showed that **20a,b** bind with moderate affinities, while **23a,b** have low affinities. **20a** exhibits higher affinity for the $\beta 2$ containing subtype than for the $\beta 4$ containing counterpart, while **20b** possesses reversed selectivity. Modeling studies suggest that the spatial distribution of the ligand's atoms around the pharmacophore elements may control their nAChR subtype selectivity.

Neuronal nAChRs hold considerable promise as therapeutic targets for the treatment of disorders of the CNS and peripheral nervous systems. Drugs aimed at nAChRs have potential for the treatment of neurodegenerative disorders, such as Alzheimer's disease, Parkinson's disease, dyskinesias, Tourette's syndrome, schizophrenia, attention deficit disorder, anxiety, and pain.^{1–3} nAChRs are ligand-gated ion channels and composed of combinations of one or more α and β subunits, and different subunit combinations define different receptor subtypes with distinct biophysical, physiological, and pharmacological properties, as well as different locations within the nervous systems. Nine α and three β subunits have been cloned, which suggests the possibility of a very large number of receptor subtypes. Although we do not yet know all the rules of assembly, based on studies of subunit mRNA and protein distribution (measured with subunit-selective antibodies), five to seven subtypes probably encompass the large majority of the nAChRs in the CNS and peripheral nervous systems. To further advance the field and to be able to better understand the different roles the subtypes play in normal physiology and pathology and to eventually exploit these receptors as potential therapeutic targets, it is important to better understand their pharmacology.

The novel alkaloid epibatidine (**1**), isolated from the Ecuadorian poisonous frog *Epipedobates tricolor*,⁴ was found to have powerful analgesic activity and high binding affinity to nAChRs.⁵ Although its high toxicity has limited its therapeutic potential, it nonetheless

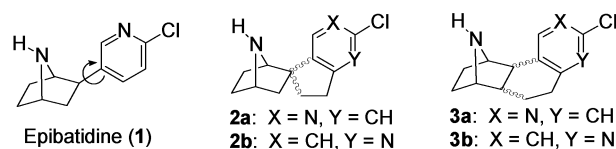
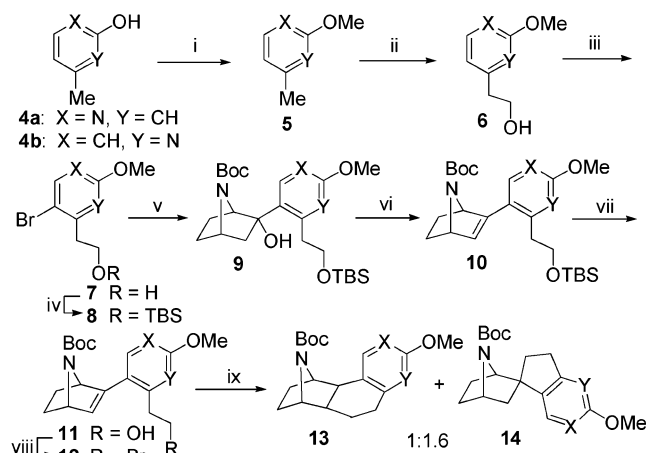


Figure 1.

Scheme 1^a



^a Reagents: (i) MeI, Ag₂CO₃, CHCl₃, 71–93%; (ii) *n*-BuLi, THF, then (CH₂O)_{*n*}, –78 °C to room temperature, 49–51%; (iii) Br₂, EtOH, 88–91%; (iv) TBSCl, imidazole, DMAP, DMF, 98%; (v) *n*-BuLi, THF, then **15**, –78 °C to room temperature, 80–86%; (vi) MsCl, Et₃N, DMAP, CH₂Cl₂, 84–87%; (vii) *n*-Bu₄NF, THF, 100%; (viii) PPh₃, CBr₄, CH₂Cl₂, 87–88%; (ix) *n*-Bu₃SnH, AIBN, toluene, reflux, 85–87%.

provides an attractive lead structure for the design of new ligands selective for distinct nAChR subtypes.^{5,6–12} Epibatidine has four low energy conformers with the internitrogen (N⁺–N) distances ranging from 4.7 to 5.5 Å due to the presence of one rotatable bond connecting the chloropyridine ring.¹³ It is uncertain which low energy conformer of epibatidine is responsible for its high affinity binding to nAChRs. The internitrogen distance related to the pharmacophore of the ligand's supposed binding conformation is still under debate.^{13–19} Therefore, the synthesis and evaluation of conformationally restricted epibatidine analogues could help in elucidating its "active" conformation on one hand and in obtaining tools to study receptor subtype selectivity on the other hand. We designed two types of conformationally constrained analogues of epibatidine, the spirocycles **2** and fused cyclic structures **3** (Figure 1). We present here our synthesis of **20a,b** and **23a,b** along with their nAChR subtype binding affinities and molecular modeling.

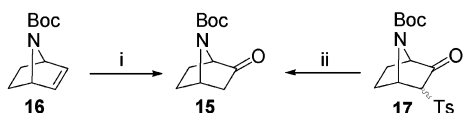
As shown in Scheme 1, our synthesis started with the commercially available **4a** or **4b**. Thus, *O*-alkylation of **4** afforded **5**, which was deprotonated with *n*-BuLi at –78 °C and quenched with paraformaldehyde to provide the primary alcohol **6**.²⁰ Selective bromination of **6** followed by protection with *tert*-butyldimethylsilyl chloride gave **8**. Treatment of the bromide **8** with *n*-BuLi at –78 °C followed by addition of ketone **15**, which could be readily prepared from **16**¹⁰ or **17**²¹ (Scheme 2), afforded the tertiary alcohol **9**. Dehydration of alcohol

* To whom correspondence should be addressed. Tel: 202-687-0686. Fax: 202-687-5065. E-mail: kozikowa@georgetown.edu.

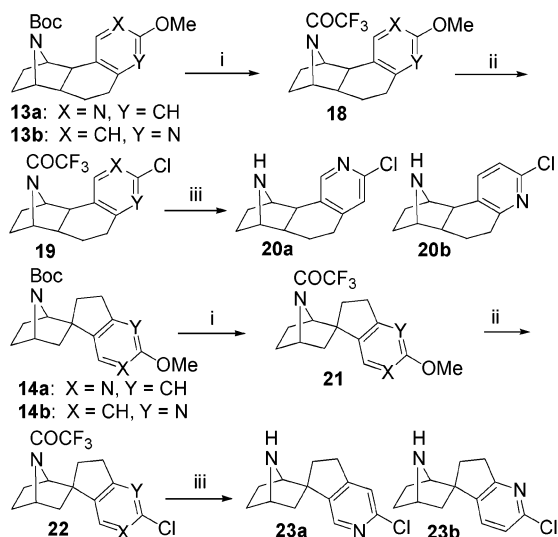
[†] Drug Discovery Program, Department of Neurology, GUMC.

[‡] Department of Pharmacology, GUMC.

[§] Naval Research Laboratory.

Scheme 2^a

^a Reagents: (i) (a) B_2H_6 , THF, then aq NaOH, 35% H_2O_2 , 46%; (b) Dess–Martin periodinane, CH_2Cl_2 , 99%; (ii) SmI_2 (2 equiv), THF–MeOH, $-78^\circ C$ to room temperature, 90%.

Scheme 3^a

^a Reagents: (i) (a) CF_3CO_2H , CH_2Cl_2 ; (b) $(CF_3CO)_2O$, pyridine, CH_2Cl_2 ; (ii) $POCl_3$, DMF, $0^\circ C$ to $95^\circ C$, 59–65%; (iii) NaOMe, MeOH, 85–96%.

9 with methanesulfonyl chloride gave the olefin **10**. Desilylation of **10** followed by treatment with PPh_3/CBr_4 furnished the bromide **12**. Radical cyclization of **12** proceeded in both the 5-*exo* and the 6-*endo* fashion to afford a 1.6:1 mixture of the spirocyclic product **14** and the fused cyclic product **13** which demonstrates that the primary radical attacked the olefin only from the *exo* face (at both the 2- and 3-positions) of the 7-azabicyclo[2.2.1]hept-2-ene moiety.

The conversion of intermediates **13a** and **13b** to the corresponding fused cyclic epibatidine analogues **20a** and **20b** is outlined in Scheme 3. Removal of the Boc group followed by reprotection as trifluoroacetamide gave **18**. Treatment of **18** under Vilsmeier conditions²² provided **19**. The trifluoroacetyl protecting group was finally removed under basic conditions to furnish the fused epibatidine analogues **20**. In the same manner, the spirocyclic epibatidine analogues **23a** and **23b** were synthesized from **14a** and **14b**, respectively (Scheme 3).

The stereochemistry of all constrained epibatidine analogues, **20a**, **20b**, **23a**, and **23b**, was confirmed by the X-ray crystallographic analysis of the intermediates **13a**, **21a**, and **21b**, and of compound **20b** itself.

Competition binding assays were carried out to measure binding affinities (K_i values) of the four compounds **20a**, **20b**, **23a**, and **23b** in their racemic forms to six defined rat nicotinic receptor subtypes expressed in stably transfected cell lines.²³ Competition curves were generated with 10 concentrations of the tested compounds against a single concentration of (\pm)- $[^3H]$ -epibatidine. K_i values were determined by nonlinear least squares regression analyses.²³ The results are

summarized in Table 1. The two spirocyclic epibatidine analogues **23a** and **23b** show relatively low binding affinities to all receptor subtypes, probably due to the orientation (*endo*) of the pyridine ring. In contrast, the two fused cyclic analogues **20a** and **20b** have much higher affinities (K_i values in nM range) for all of the receptor subtypes, though they are still significantly lower than those of epibatidine (**1**). It is interesting to note that for each $\alpha\beta$ subunit combination representing a potential receptor subtype, **20a** exhibits higher affinity for the β_2 containing subtype than for the β_4 containing counterpart. This pattern of higher affinity for β_2 containing receptors is similar to most known nicotinic ligands. In contrast, **20b** possesses higher affinities for the β_4 containing subtype than for the β_2 containing counterpart. This is an unusual, if not unique, pattern of selectivity among all nicotinic ligands that possess moderate to high affinities for β_2 and β_4 containing nicotinic receptor subtypes.

To understand the moderate affinities of the ligands **20a** and **20b** and the low affinities of **23a** and **23b**, the pharmacophore elements of **23a** and **23b** were compared to those of **20a**, **20b**, and epibatidine (**1**), employing an improved pharmacophore model that has been proposed for the nAChR binding site.^{16,17} The ligands **20a**, **20b**, **23a**, and **23b** were subjected to conformational analysis using the *Advanced calculations* module in Sybyl.²⁴ It was found that **20a** and **20b** have two stable conformations with a ΔE of less than 3 kcal/mol distinguished by the conformation of the central six-membered ring (twist 1: **20a1** and **20b1**, and twist 2: **20a2** and **20b2**). There were no additional conformations found for **23a** and **23b** since the other possible “envelop” conformation of the central five-membered ring of **23a** and **23b** is unstable due to an unfavorable interaction of H^b and H^c (Table 2). The analysis of the RMS fit has shown that the calculated conformations **20a2**, **20b1**, **23a**, and **23b** are almost identical to the X-ray structures of **13a**, **20b**, **21a**, and **21b**, respectively (RMS values < 0.14 Å).

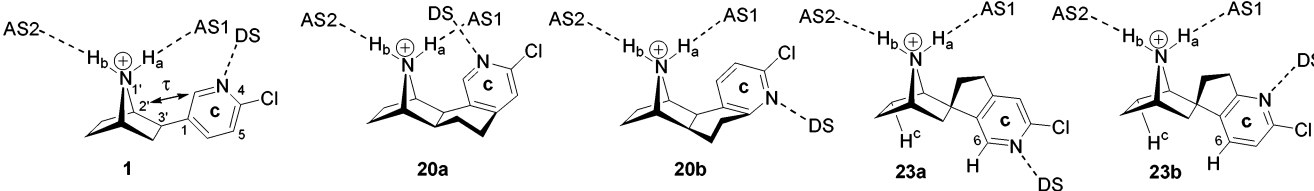
Although several stable low energy conformations are known for epibatidine (**1**), for our study we used only one conformation that is believed to interact with nAChRs ($\tau = 7^\circ$).¹³ Two possible acceptor sites in the binding site of the nAChR that are able to interact with the charged hydrogen atoms H_a and H_b are marked as AS1 and AS2 (Table 2).

A potential hydrogen donor site in the binding site that is able to interact with the pyridine nitrogen is marked as DS. The acceptor sites and donor site were placed 2.9 Å from the corresponding atoms in **20a**, **20b**, **23a**, and **23b** (Table 2) using the defaults settings for acceptor and donor sites in UNITY.²⁴ The centroid of the pyridine ring was defined as “c”. The pharmacophore elements defined by Tønder et al.¹⁷ consist of the distances between the acceptor and donor sites, the distances between the acceptor sites and centroid c, and the angle formed by centroid c and either one of the acceptor sites AS1 or AS2, and the donor site DS. The pharmacophore parameters obtained for epibatidine (**1**) match the parameters reported by Tønder et al.¹⁷ In all ligands the distance between the charged aliphatic nitrogen and the pyridine nitrogen ranges between 4.9 and 5.9 Å, which is consistent with the observation that the internitrogen distance (N^+-N) in active nAChR

Table 1. Binding Affinities (K_i , nM) of (-)-Nicotine, (\pm)-Epibatidine, and Four Constrained Epibatidine Analogues to Six nAChR Subtypes^a

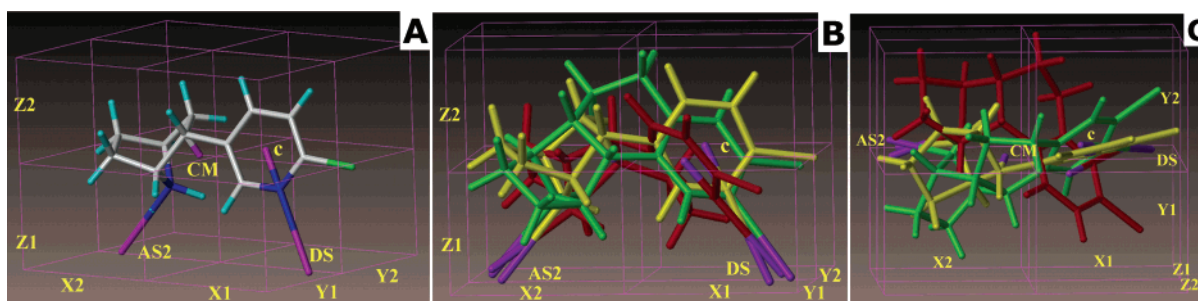
ligand	$\alpha 2\beta 2$	$\alpha 2\beta 4$	$\alpha 3\beta 2$	$\alpha 3\beta 4$	$\alpha 4\beta 2$	$\alpha 4\beta 4$
nicotine	12 \pm 2	112 \pm 21	47 \pm 11	443 \pm 60	10 \pm 2	40 \pm 6
1	0.025 \pm 0.001	0.095 \pm 0.017	0.035 \pm 0.011	0.565 \pm 0.121	0.061 \pm 0.009	0.157 \pm 0.006
20a	290 \pm 5	717 \pm 36	354 \pm 10	2280 \pm 220	73 \pm 11	637 \pm 302
20b	59 \pm 7	32 \pm 3	530 \pm 81	201 \pm 16	295 \pm 85	41 \pm 14
23a	12600 \pm 5300	10700 \pm 1000	19700 \pm 4500	14900 \pm 4500	29200 \pm 4300	10500 \pm 4500
23b	2690 \pm 230	7180 \pm 190	4070 \pm 850	13800 \pm 1700	6990 \pm 2000	9460 \pm 3700

^a K_d values (nM) for [³H]-epibatidine used for calculating K_i values were 0.02 for $\alpha 2\beta 2$, 0.08 for $\alpha 2\beta 4$, 0.03 for $\alpha 3\beta 2$, 0.30 for $\alpha 3\beta 4$, 0.04 for $\alpha 4\beta 2$, and 0.09 for $\alpha 4\beta 4$ (Xiao and Kellar, 2003, manuscript in preparation). The K_i values of (-)-nicotine and epibatidine (**1**) shown were the mean \pm SEM of three to six independent measurements. The K_i values of **20a,b** and **23a,b** shown were the mean \pm SEM of three independent measurements.

Table 2. Comparison of the Pharmacophore Fingerprints in Epibatidine (**1**) and Constrained Analogues of Epibatidine **20a,b** and **23a,b**. RMS Fit Values between **20a,b** and **23a,b** and the X-ray Structures of **13a**, **20b**, **21a**, and **21b**, Respectively^a


compound	$d(N^+-N)$ (Å)	$d(AS1-DS)$ (Å)	$d(AS2-DS)$ (Å)	$d(AS1-c)$ (Å)	$d(AS2-c)$ (Å)	$\Delta(c-AS1-DS)$ (deg)	$\Delta(c-AS2-DS)$ (deg)	total energy ^b	RMS fit (Å) ^c
pharm model ^d	4.5–6.0	7.3–8.0		6.5–7.4		30–36 ^e			
1 ^f	4.7	4.6	7.8	3.7	7.0	64	34	32.4	
20a1	4.9	6.6	9.1	3.0	6.4	33	26	31.7	0.47
20a2	5.0	6.3	8.7	3.6	6.9	42	30	32.7	0.07
20b1	4.4	4.0	8.4	2.9	6.4	77	31	31.1	0.13
20b2	5.1	5.6	9.9	3.6	6.9	52	23	32.0	0.44
23a	5.9	10.4	10.1	6.7	7.5	16	23	38.1	0.10
23b	5.9	8.5	10.2	6.7	7.5	30	23	38.0	0.10

^a Compounds **20a**, **20b**, **23a**, and **23b** are rendered in the conformations found in the X-ray structures of **13a**, **20b**, **21a**, and **21b**, respectively. ^b Total energy calculated using Tripos Force Field. ^c Pairwise RMS values between the heavy atoms of the calculated conformers and the corresponding atoms in their X-ray structures. For compounds **20a**, **23a**, and **23b** only matching atoms were used to calculate the RMS values. The structures were aligned using the least-squares fit algorithm implemented in Sybyl. ^d Tønder et al.¹⁷ ^e Rounded, the original values in ref 17 are 30.4° and 35.8°. ^f τ ($\angle 2'-3'-1-2$) is 4°, minimization by Tripos Force Field may be responsible for the difference between our results and the results obtained by Tønder et al.¹⁷

**Figure 2.** (A) Alignment of epibatidine **1** (rendered as colored stick model) in a rectangular box measuring $10 \times 8 \times 7 \text{ \AA}^3$ (rendered by violet lines). Carbon atoms are colored gray, hydrogen cyan, nitrogen blue, chlorine green. Acceptor site AS2, donor site DS, centroid "c", and center of mass CM are rendered by violet sticks. (B) Overlay of **1** rendered as yellow stick model, **20a2** rendered as green model, and **20b1** rendered as red model in the rectangular box. (C) Another projection of the models shown in the panel B.

ligands should extend from 4.5 to 6.0 Å.¹⁶ Comparison of the pharmacophore parameters derived from the two conformations of ligands **20a** and **20b** reveals that conformations **20a2** and **20b1** exhibit the best match with the pharmacophore model proposed by Tønder et al. (Table 2).¹⁷ Moreover, none of the pharmacophore parameters derived from acceptor site AS1 has a match with the pharmacophore model. This may indicate that only hydrogen H_b is required for binding, whereas the hydrogen H_a is redundant and the position of H_a can be used for further modification of the ligands **20a** and **20b**. Interestingly, the distance AS2–c and the angle

c–AS2–DS in conformers **20a2** and **20b1** are within the allowed range of 6.5–7.4 Å and 30–36°, whereas the distance AS2–DS is 0.7 Å (in **20a2**) and 0.4 Å (in **20b1**) larger than the maximum distance allowed by the pharmacophore model.¹⁷ To determine how well these ligands overlay with each other, both nitrogen atoms, acceptor site AS2, and donor site DS of epibatidine (**1**), **20a2**, and **20b1** were aligned using the least-squares fit algorithm implemented in Sybyl (Figure 2B,C). The pairwise RMS values are 0.44 Å for **1** and **20a2**, and 0.51 Å for **1** and **20b1**. These deviations are large enough to weaken the putative hydrogen bonds

or ionic interactions between these ligands and the binding site, suggesting that the larger than 8.0 Å distance AS2–DS may be responsible for the moderate affinities of **20a** and **20b** in comparison to the affinities of epibatidine (**1**). To compare the projections of ligands **1**, **20a**, and **20b** to the space surrounding the pharmacophore elements, these ligands were enclosed in a rectangular box measuring $10 \times 8 \times 7 \text{ \AA}^3$ (Figure 2B,C). The box was split into eight equal smaller rectangular boxes by planes dividing each side of the box into half. Ligand **1** was placed inside the box so that the pharmacophore elements AS2 and DS were located on the bottom of the box and on the line dividing the box into the Y1 and Y2 halves (sectors) simultaneously, whereas the center of mass of ligand **1** and centroid **c** were located in the plane dividing the box into sectors Y1 and Y2 (Figure 2A). After that, the ligands **20a** and **20b** were overlaid on ligand **1** as described above. As a result, the aromatic rings of all ligands are located in the sector X1 and the 7-azabicyclo[2.2.1]heptane moieties of all ligands are located in the sector X2. Comparison of **1**, **20a**, and **20b** shows that the 7-azabicyclo[2.2.1]heptane moiety of **20a** projects into the sector Y1, whereas this moiety in **20b** is located mostly in the sector Y2. Five out of seven heavy atoms of the pyridine ring (carbons 4, 5, 6, nitrogen 3, and chlorine) in **20a** project into the sector Y2, whereas the same five atoms in **20b** project into the sector Y1. Interestingly, all atoms of the middle ring of **20a** are located in sector Z2, whereas only two atoms in the middle ring of **20b** are located in sector Z2, the rest of them projecting into sector Z1. Therefore, despite the good match among the pharmacophore elements of epibatidine (**1**) and the ligands **20a** and **20b**, enough differences exist that may explain their dissimilar selectivity profiles.

The low affinities found for ligands **23a** and **23b** are consistent with the large differences in the pharmacophore parameters derived from these ligands and the optimum values determined by Tønder et al. (Table 2).¹⁷

Acknowledgment. We thank Haizhu P. Wang and Maryna Baydyuk for their assistance with tissue culture and ligand binding assays. This work was supported by the National Institutes of Health (DA06486 and DA12976) and by the National Institute of Mental Health through the Psychoactive Drug Screening Program (N01MH80005).

Supporting Information Available: Crystal data for compounds **13a**, **20b**, **21a**, and **21b**, and detailed experimental procedures with spectroscopic data. This material is available free of charge via the Internet at <http://pubs.acs.org>.

References

- Lindstrom, J. Nicotinic acetylcholine receptors in health and disease. *Mol. Neurobiol.* **1997**, *15*, 193–222.
- Paterson, D.; Nordberg, A. Neuronal nicotinic receptors in the human brain. *Progr. Neurobiol.* **2000**, *61*, 75–111.
- Lloyd, G. K.; Williams, M. Neuronal nicotinic acetylcholine receptors as novel drug targets. *J. Pharmacol. Exp. Ther.* **2000**, *292*, 461–467.
- Spande, T. F.; Garraffo, H. M.; Edwards, M. W.; Yeh, H. J. C.; Pannell, L.; Daly, J. W. Epibatidine: A novel (chloropyridyl)-azabicycloheptane with potent analgesic activity from an Ecuadorian poison frog. *J. Am. Chem. Soc.* **1992**, *114*, 3475–3478.
- Holladay, M. W.; Dart, M. J.; Lynch, J. K. Neuronal nicotinic acetylcholine receptors as targets for drug discovery. *J. Med. Chem.* **1997**, *40*, 4169–4194.
- Carroll, F. I.; Lee, J. R.; Navarro, H. A.; Ma, W.; Brieady, L. E.; Abraham, P.; Damaj, M. I.; Martin, B. R. Synthesis, nicotinic acetylcholine receptor binding, and antinociceptive properties of 2-*exo*-2-(2', 3'-disubstituted 5'-pyridinyl)-7-azabicyclo[2.2.1]-heptanes: epibatidine analogues. *J. Med. Chem.* **2002**, *45*, 4755–4761.
- Gohlke, H.; Gundisch, D.; Schwarz, S.; Seitz, G.; Tilotta, M. C.; Wegge, T. Synthesis and nicotinic binding studies on enantiopure diazine analogues of the novel (2-chloro-5-pyridyl)-9-azabicyclo[4.2.1]non-2-ene UB-165. *J. Med. Chem.* **2002**, *45*, 1064–1072.
- Sharples, C. G. V.; Karig, G.; Simpson, G. L.; Spencer, J. A.; Wright, E.; Millar, N. S.; Wonnacott, S.; Gallagher, T. Synthesis and pharmacological characterization of novel analogues of the nicotinic acetylcholine receptor agonist (±)-UB-165. *J. Med. Chem.* **2002**, *45*, 3235–3245.
- Cheng, J.; Zhang, C.; Stevens, E. D.; Izenwasser, S.; Wade, D.; Chen, S.; Paul, D.; Trudell, M. L. Synthesis and biological evaluation at nicotinic acetylcholine receptors of *N*-aryllalkyl- and *N*-aryl-7-azabicyclo[2.2.1]heptanes. *J. Med. Chem.* **2002**, *45*, 3041–3047.
- Carroll, F. I.; Liang, F.; Navarro, H. A.; Brieady, L. E.; Abraham, P.; Damaj, M. I.; Martin, B. R. Synthesis, nicotinic acetylcholine receptor binding, and antinociceptive properties of 2-*exo*-2-(2'-substituted 5'-pyridinyl)-7-azabicyclo[2.2.1]heptanes. Epibatidine analogues. *J. Med. Chem.* **2001**, *44*, 2229–2237.
- Carroll, F. I.; Lee, J. R.; Navarro, H. A.; Brieady, L. E.; Abraham, P.; Damaj, M. I.; Martin, B. R. Synthesis, nicotinic acetylcholine receptor binding, and antinociceptive properties of 2-*exo*-2-(2'-substituted-3'-phenyl-5'-pyridinyl)-7-azabicyclo[2.2.1]heptanes. Novel nicotinic antagonists. *J. Med. Chem.* **2001**, *44*, 4039–4041.
- Cox, C. D.; Malpass, J. R.; Gordon, J.; Rosen, A. Synthesis of epibatidine isomers: *endo*-5- and 6-(6'-chloro-3'-pyridyl)-2-azabicyclo[2.2.1]heptanes. *J. Chem. Soc., Perkin Trans. 1* **2001**, 2372–2379.
- Tønder, J. E.; Hansen, J. B.; Begtrup, M.; Pettersson, I.; Rimvall, K.; Christensen, B.; Ehrbar, U.; Olesen, P. H. Improving the nicotinic pharmacophore with a series of (isoxazole)methylene-1-azacyclic compounds: synthesis, structure–activity relationship, and molecular modeling. *J. Med. Chem.* **1999**, *42*, 4970–4980.
- Lee, M.; Dukat, M.; Liao, L.; Flammia, D.; Damaj, M. I.; Martin, B.; Glennon, R. A. A comparison of the binding of three series of nicotinic ligands. *Bioorg. Med. Chem. Lett.* **2002**, *12*, 1989–1992.
- Brown, L. L.; Kulkarni, S.; Pavlova, O. A.; Koren, A. O.; Mukhin, A. G.; Newman, A. H.; Horti, A. G. Synthesis and evaluation of a novel series of 2-chloro-5-((1-methyl-2-(*S*-pyrrolidinyl)methoxy)-3-(2-(4-pyridinyl)vinyl)pyridine analogues as potential positron emission tomography imaging agents for nicotinic acetylcholine receptors. *J. Med. Chem.* **2002**, *45*, 2841–2849.
- Tønder, J. E.; Olesen, P. H. Agonists at the $\alpha 4\beta 2$ nicotinic acetylcholine receptors: structure–activity relationships and molecular modelling. *Curr. Med. Chem.* **2001**, *8*, 651–674.
- Tønder, J. E.; Olesen, P. H.; Hansen, J. B.; Begtrup, M.; Pettersson, I. An improved nicotinic pharmacophore and a stereoselective CoMFA-model for nicotinic agonists acting at the central nicotinic acetylcholine receptors labeled by [³H]-*N*-methylcarbamylcholine. *J. Comput.-Aided Mol. Des.* **2001**, *15*, 247–258.
- Koren, A. O.; Horti, A. G.; Mukhin, A. G.; Gündisch, D.; Kimes, A. S.; Dannals, R. F.; London, E. D. 2-, 5-, and 6-Halo-3-(2(*S*)-azetidylmethoxy)pyridines: synthesis, affinity for nicotinic acetylcholine receptors, and molecular modeling. *J. Med. Chem.* **1998**, *41*, 3690–3698.
- Glennon, R. A.; Herndon, J. L.; Dukat, M. Epibatidine-aided studies toward definition of a nicotinic receptor pharmacophore. *Med. Chem. Res.* **1994**, *4*, 461–473.
- Brodne, M. A.; Padwa, A. Electrophilic aromatic substitution on pyridine rings. Intramolecular cyclization using *N*-acyliminium ions. *Tetrahedron Lett.* **1997**, *38*, 6153–6156.
- Zhang, C.; Ballay, C. J., II; Trudell, M. L. 2-Bromoethynyl aryl sulfones as versatile dienophiles: a formal synthesis of epibatidine. *J. Chem. Soc., Perkin Trans. 1* **1999**, 675–676.
- Sirisoma, N. S.; Johnson, C. R. α -Iodocycloalkenones: synthesis of (±)-epibatidine. *Tetrahedron Lett.* **1998**, *39*, 2059–2062.
- Xiao, Y.; Meyer, E. L.; Thompson, J. M.; Surin, A.; Wroblewski, J.; Kellar, K. J. Rat $\alpha 3\beta 4$ subtype of neuronal nicotinic acetylcholine receptor stably expressed in a transfected cell line: pharmacology of ligand binding and function. *Mol. Pharmacol.* **1998**, *54*, 322–333.
- Sybyl, 6.8 ed.; UNITY, 4.3 ed.; Tripos Inc.: 1699 South Hanley Rd., St. Louis, MO 63144.